

Numerical Simulation of Generalized Power Law Blood Flow Model Through Different Angles of Stenosed Bifurcated Artery

Azyante Erma Abd Aziz ¹, Muhammad Sabaruddin Ahmad Jamali ², Zuhaila Ismail^{3*}

^{1,2,3} Department of Mathematical Sciences, Faculty of Science, Universiti Teknologi Malaysia,
81310, Johor Bahru, Malaysia.

*zuhaila@utm.my

Abstract: Atherosclerosis is a key occurrence in cardiovascular disease and is the leading cause of death for people worldwide. Atherosclerosis is the narrowing of lumen as a result of plaque deposition which is known as stenosis. Therefore, arteries become constricted as the stenosis continues to enlarge. These conditions will disturb blood flow where the eddies and separation of streamlines near the vessel wall are formed. The study of numerical simulation of generalized power law for non-newtonian model through different angles of a bifurcated artery is considered in this paper. Realizing that the characteristics of blood influence vascular disease, this study was conducted to acquire knowledge on blood flow characteristics such as velocity profile, pressure drop, streamlines and wall shear stress on different angles of stenosed bifurcated artery. Angles of stenosed bifurcated arteries were divided into three: $\beta=150$, $\beta=300$, and $\beta=600$; to study the effect of different angles of stenosed bifurcated artery through a single stenosis. Results were obtained using COMSOL Multiphysics 5.2 which was based on finite element method in two-dimensional (2D) blood flow model in the presence of single stenosis with different angles of stenosed bifurcated artery.

Keywords: Bifurcated artery, Blood flow, COMSOL, Generalized power law, Stenosis.

1 Introduction

World Health Organization (WHO) has confirmed that cardiovascular diseases (CVDs) are the world's biggest killer which accounted for more people dead annually compared to any other causes. An estimated number of people dead is 17 million deaths per year, representing 85% of death caused by malfunction of organ, heart attack and stroke, Huh [1]. In order to understand and discover the genesis of this vascular disease, special attention and interest have been given by many researchers all around the world. Cardiovascular diseases, such as heart attack and stroke, are caused by atherosclerosis. The atherosclerosis lesion is one of the most widespread diseases in human beings that can lead to death, Zain [2]. Coronary artery disease is caused by atherosclerosis that occurred due to stenosis which is formed as a result of fatty substances, cholesterol, cellular waste products, and smooth muscle cells accumulation on the arterial wall, Zaman [3]. Besides, there is evidence that shows early onset of atherosclerosis may lead to changes in vessel wall size and deposition of platelet thrombi will occur near the branching entrance. These conditions will disturb blood flow which, from a fluid mechanical point of view, can be related to the formation of eddies and separation of streamlines near vessel wall, Genuardi [4]. In order to study blood flow behaviour in the coronary artery, various mathematical models have been developed based on artery geometry, fluid types, stenosis shape and location, initial and boundary conditions, and external forces effects. A detailed evaluation on the numerical computation of generalized power law model of different angles of stenosed bifurcated artery are performed. In many studies, the geometry of stenosis is expected to be smooth and is represented by a smooth curve. In general, they may be classified as single or mild, double and multiple stenoses. It is common to see that single stenosis is also called mild stenosis even though a mild stenosis can

progress to severe stenosis as the height of stenosis increases. The presence of single stenosis in the blood flow has been detected in many studies as it is the best state of stenosis to start off with and acts as a benchmark for further studies as an improvement for the problem.

In general, blood does not exhibit a constant viscosity at all flow rates, especially non-Newtonian fluid type in the microcirculatory system. The non-Newtonian behaviour is more realistic at a very low shear rates as red blood cells clump together into larger particles, Ku [5]. The blood cells start to characterize as a non-Newtonian fluidic in small vessels where the cell-free skimming layer reduces effective viscosity through the tube. Besides that, work by Rabby et al. [6] shows the five types of non-Newtonian, which are Casson model, Carreau model, generalized power law model, Walburn-Schneck model. They conducted a study on blood flow through four different right coronary arteries, which have been reconstructed from bi-plane angiograms, and concluded that generalised power law model was to be used in order to achieve better approximation of wall shear stress at low shear. The significance of Newtonian and non-Newtonian blood model such as Carreau model, Walburn-Schneck model, power law, Casson model and generalized power law model was investigated by Johnston et al. [7]. The result shows a low central velocity inlet and wall shear stress values of Newtonian model are lower than those of non-Newtonian. High central velocity inlet and wall shear stress value of Newtonian and non-Newtonian are nearly identical. Sarifuddin [8] studied the shear-thickening and shear-thinning of the generalized power law model in an artery with different kinds of stenosis i.e. cosine, smooth-shaped constrictions and irregular without any body force.

To date, there are quite a number of studies concerning inclined angle in single channel of blood flow such as Kumari [9]. They studied the peristaltic pumping of a Casson model in an inclined channel under the effect of a magnetic field. In 2013, they improved the study by proposing mathematical modelling and numerical solution for the flow of a micropolar fluid under the effect of magnetic field in an inclined channel under the considerations of low Reynolds number. Biswas [10] investigated the steady flow of blood (Newtonian fluid) through an inclined tapered constricted artery with an axial slip in velocity at the tapered vessel wall. The analysis included Poiseuille flow of blood, one-dimensional blood flow models through uniformed and tapered vessels with or without narrowing, with a slip or zero-slip cases and for straight or inclined geometries, as its special cases. Verma [11] studied one-dimensional blood flow in a rigid inclined circular tube subjected to external magnetic field. A study was conducted by Biswas [12] on blood flow through an inclined tube with a slip at the stenotic wall. They found that the velocity of blood flow increases as the inclination angle of the tube increases. This present study mainly focuses on laminar flow through different angles of bifurcated artery with generalized power law model of blood flow. The simulation result was obtained using COMSOL Multiphysics 5.2, a software based on the FEM.

2 Problem Formulation

In order to formulate the computational domain for the stenosed bifurcated artery, these following assumptions are imposed:

1. The artery forming bifurcation is of finite length.
2. The parent aorta possesses a single mild shaped stenosis in its lumen.
3. Curvatures are introduced at the lateral junctions and the flow divider of the arterial bifurcation to ensure that one can rule out the presence of any discontinuity causing the non-existence of separation zones.

A Model construction

The geometry of the stenosed bifurcated artery is modelled as a bifurcated channel as proposed by Jamali and Ismail [13], and Chakravarty [14]. Let the coordinates be of a material point. The outer and inner wall geometry is described by

$$R_1(x) = \begin{cases} a, 0 \leq x \leq d, d + l_0 \leq x \leq x_1 \\ a - \frac{4\tau_m}{l_0^2} (l_0(x-d) - (x-d)^2), d \leq x \leq d + l_0 \\ a + r_0 - \sqrt{r_0^2 - (x-x_1)^2}, x_1 \leq x \leq x_2 \\ 2r_1 \sec \beta + (x-x_2) \tan \beta, x_2 \leq x \leq x_{\max} - s \end{cases} \quad R_2(x) = \begin{cases} 0, & 0 \leq x \leq x_3, \\ \sqrt{r_0' - (x - (x_3 + r_0'))^2}, & x_3 \leq x \leq x_4, \\ r_0' \cos \beta + (x-x_4) \tan \beta, & x_4 \leq x \leq x_{\max} \end{cases}$$

where a and r_1 are the radii of the mother and daughter artery, respectively. r_0 and r_0' are the radii of curvature for the lateral junction, l_0 is the length of the stenosis at a distance d . x_1 and x_2 are the location of the onset and offset of the lateral junction, x_3 as the apex, τ_m is the maximum height of stenosis at $d + l_0 / 6$ and $d + 5l_0 / 6$, β is half of the bifurcation angle.

$$x_2 = x_1 + r_0 \sin \beta, r_0 = (a - 2r_1 \sec \beta) / (\cos \beta - 1), r_0' = (x_3 - x_2) \sin \beta / (1 - \sin \beta).$$

$$x_3 = x_2 + q, s = 2r_1 \sin \beta, x_4 = x_3 + r_0' (1 - \sin \beta)$$

where q is taken as a small number lying in the range of $0.001 \leq q \leq 0.005$ chosen for the compatibility of the geometry.

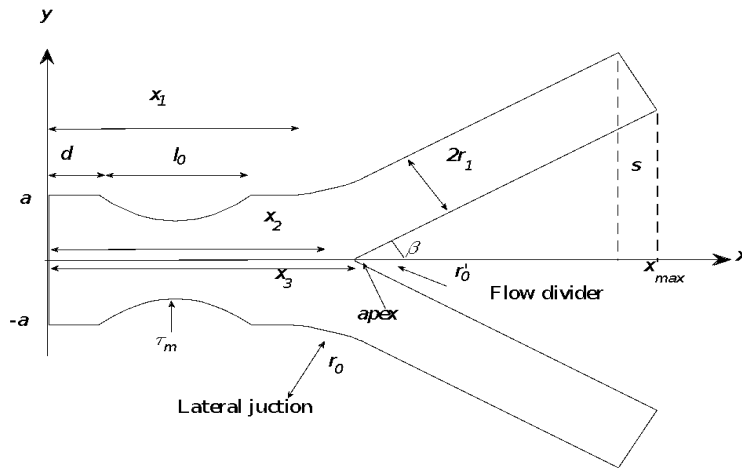


Figure 1: The two-dimensional schematic model of mild stenosis in bifurcated artery

3 The Governing Equation

The streaming fluid representing blood in the arterial bifurcation is generally considered to be laminar and followed the non-Newtonian Generalized Power law characteristic of fluid rheology. The governing equation of incompressible flow is given by

$$\frac{\partial u}{\partial x} + \frac{\partial v}{\partial y} = 0 \quad (1)$$

$$\rho \left(u \frac{\partial u}{\partial x} + v \frac{\partial u}{\partial y} \right) = -\frac{\partial p}{\partial x} + \left(\frac{\partial \tau_{xx}}{\partial x} + \frac{\partial \tau_{yx}}{\partial y} \right) \quad (2)$$

$$\rho \left(u \frac{\partial v}{\partial x} + v \frac{\partial v}{\partial y} \right) = -\frac{\partial p}{\partial y} + \left(\frac{\partial \tau_{xy}}{\partial x} + \frac{\partial \tau_{yy}}{\partial y} \right) \quad (3)$$

with,

$$\begin{aligned} \bar{\tau} &= - \left\{ m \left[\sqrt{\frac{1}{2} (\underline{\Delta} : \underline{\Delta})} \right]^{n-1} \right\} \underline{\Delta} \\ \tau_{xx} &= -2 \left\{ m \left[\left[\frac{1}{2} (\underline{\Delta} : \underline{\Delta}) \right]^{1/2} \right]^{n-1} \right\} \left(\frac{\partial u}{\partial x} \right), \\ \tau_{yy} &= -2 \left\{ m \left[\left[\frac{1}{2} (\underline{\Delta} : \underline{\Delta}) \right]^{1/2} \right]^{n-1} \right\} \left(\frac{\partial v}{\partial y} \right), \\ \tau_{xy} = \tau_{yx} &= - \left\{ m \left[\left[\frac{1}{2} (\underline{\Delta} : \underline{\Delta}) \right]^{1/2} \right]^{n-1} \right\} \left(\frac{\partial v}{\partial x} + \frac{\partial u}{\partial y} \right), \end{aligned}$$

where $\underline{\Delta}$ is the strain rate tensor and m is the fluid consistency coefficient and n is flow behaviour index. $\bar{\tau}$ is the stress tensor, u is the axial velocity, v is the radial velocity, y is the radial coordinate and x is axial coordinate. μ denotes the dynamic viscosity of blood, ρ is the density of blood, and P is the pressure distribution acting on the surface.

4 Boundary Conditions

At the inlet, a parabolic velocity profile is imposed as:

$$u(x, y) = u_{\max} \left(1 - \left(\frac{y^2}{a^2} \right)^{\frac{n+1}{n}} \right) \text{ and } v(x, y) = 0, \text{ at } x = 0, \text{ and } -a \leq y \leq a. \quad (4)$$

No-slip conditions along all the arterial walls

$$u(x, y) = 0, v(x, y) = 0. \quad (5)$$

A traction-free condition is applied at the outlet which can be stated as

$$(-p\mathbf{I} + \tau) \cdot \mathbf{n} = 0, \quad (6)$$

where \mathbf{n} represents a unit outward normal vector with the pressure point constraint, $p = 0$ being implemented at $x = 0$ and $y = 0.0075$.

A Computational Mesh and Validation

The governing equations (1)-(3), subjected to the boundary conditions (4)-(6) mentioned above, are solved by using the commercial software package, COMSOL Multiphysics 5.2. All computations were performed on a personal computer running 64-bit Windows 8 with speed of 1.70GHz and a RAM of 9.89GB. The geometry was drawn by means of the built-in CAD tools. Then, the built-in meshing function was used to generate unstructured triangular elements of the model. Several attempts of mesh are performed in COMSOL Multiphysics to ensure the results obtained were not dependent on the mesh parameters (see Figure 2 and Figure 3). The number of domain elements and maximum velocity computed using COMSOL Multiphysics in the present study are summarised in Table 1.

Table 1: Mesh Parameters Computed in COMSOL Multiphysics and Matlab

Software	Parameter	Domain elements	Maximum velocity (m/s)
Present study, COMSOL	mesh 1	2423	0.04560
	mesh 2	7258	0.04531
	mesh 3	17753	0.04529
	mesh 4	20083	0.04555

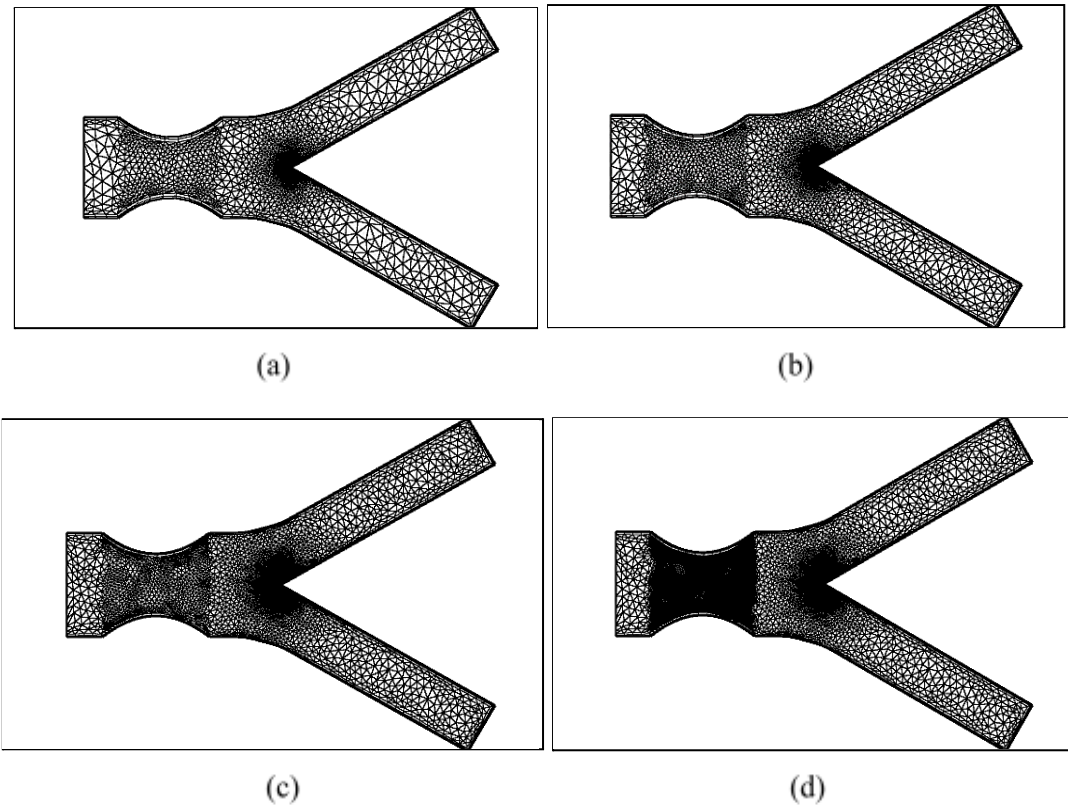


Figure 2: Unstructured Triangular Mesh Elements (a) Mesh 1; (b) Mesh 2; (c) Mesh 3; and (d) Mesh 4

Based on the mesh dependency test demonstrated in Table 1 and Figure 3, maximum velocity for all mesh are nearly identical (refer dotted box in Figure 3). Therefore, mesh 3, with domain element 17753, is selected in order to provide a satisfactory solution to the problem. These results agree with Zain [15]. Then, a similar step of meshing process is performed for the problem of different angles of bifurcation.

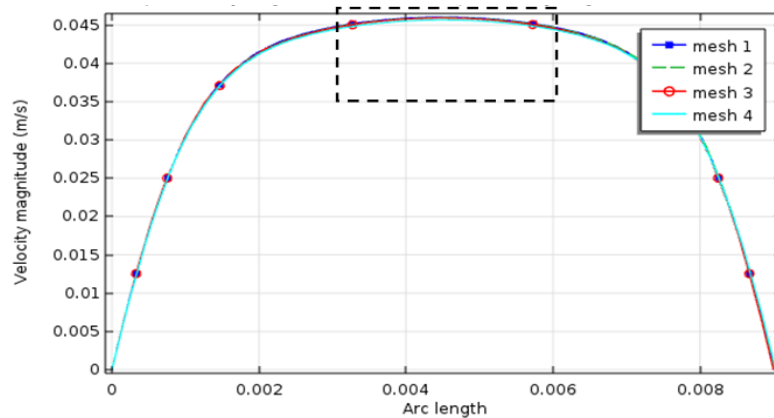


Figure 3 : Axial Velocity Profiles for Different Number of Domain Elements at $x = 0.0125\text{m}$ by using COMSOL Multiphysics

5 Simulations And Results

The simulation performed in order to estimate the velocity profiles, pressure and streamline through different value angles of bifurcated, β , has been proposed by Srinivasacharya [16]. The blood flow behaviour used the three value of angles, which were $\beta = \frac{\pi}{12} = 15^\circ$, $\beta = \frac{\pi}{12} = 30^\circ$, and $\beta = \frac{\pi}{12} = 60^\circ$.

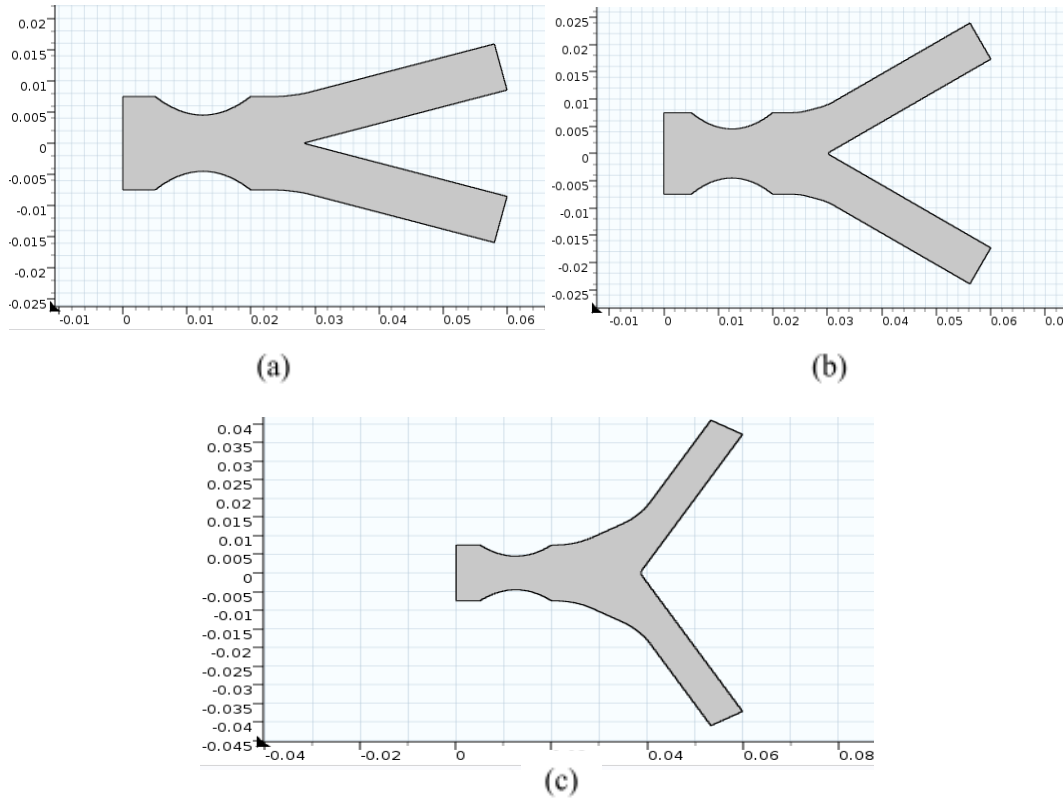


Figure 4: Model of Bifurcated Artery with the Angles of, (a) $\beta = 15^\circ$; (b) $\beta = 30^\circ$; and (c) $\beta = 60^\circ$

To have a thorough quantitative analysis on the effects of generalized power law of blood rheology on the stenotic bifurcated artery flow phenomenon, the parameter values were adopted from [13], [14] i.e.

$$a = 0.0075\text{m}, l_0 = 0.015\text{m}, d = 0.005\text{m}, x_{\max} = 0.06\text{m}, x_1 = 0.025\text{m}, \rho = 1050\text{kgm}^{-3}, \mu = 0.0035\text{Pas}^{-1},$$

$$q = 0.002\text{m}, r_1 = 0.51a, l_0 = 0.015\text{m}, d = 0.005\text{m}, x_{\max} = 0.06\text{m}, x_1 = 0.025\text{m}, \tau_m = 0.4a.$$

A Velocity Profiles Results

In this section, the discussion regarding the effects of different angles, β , of stenosed bifurcated artery on velocity profile will be carried out. Figure 5 indicates how the different angles of stenosed bifurcated artery, β , affects the velocity magnitude at $x = 0.0125m$. Based on the figure, the velocity magnitude for 60 degrees of angle of the stenosed bifurcated artery is the lowest at 0.0462542m/s velocity magnitude, followed by 30 degrees of angle and 15 degrees of angle. Result of 30 degrees of angle shows the velocity magnitude at 0.0464009 m/s while for 15 degrees of angle shows 0.0466028 m/s velocity magnitude.

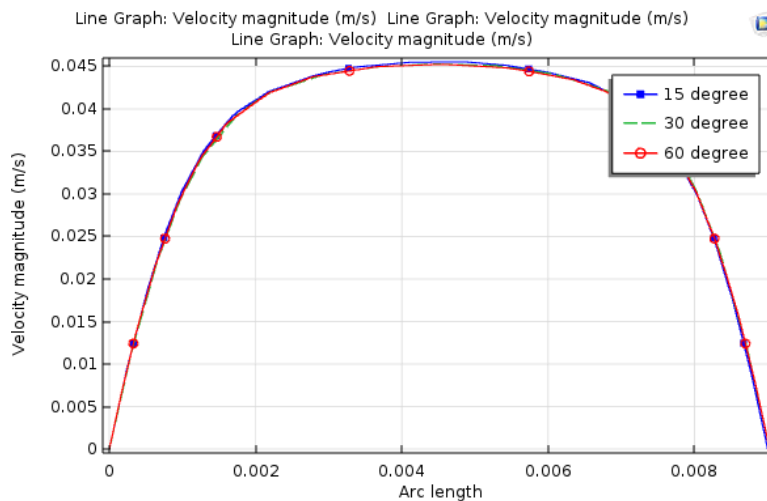


Figure 5: The Different Sngles of Stenosed Bifurcated Artery Affects the Velocity Magnitude at $x = 0.0125m$.

The results further explained that increasing the angle of stenosed bifurcated artery, will decrease the magnitude of velocity. Figure 6 (a) shows the velocity magnitude at minimum (0.000 m/s) and maximum velocity magnitude at 0.0466028 m/s at $\beta = 15^{\circ}$. The results further support the finding that the higher angles of stenosed bifurcated artery will result in a decrease in velocity magnitude. Furthermore, Figure 6 (b) shows the decreasing velocity magnitude at 0.0464009 m/s at $\beta = 30^{\circ}$ while with the highest angle of stenosed bifurcated artery (at $\beta = 60^{\circ}$) shows the slight increase of velocity magnitude at 0.0462542 in Figure 6 (c).

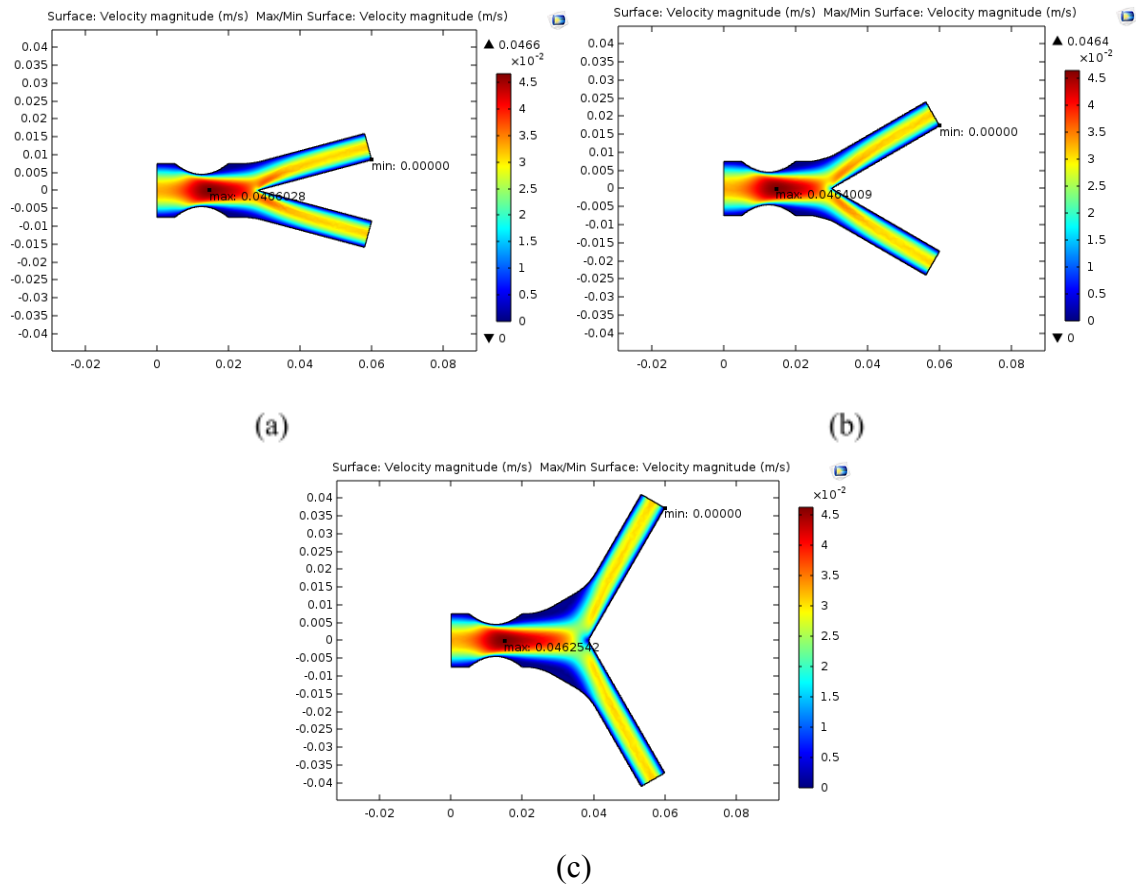


Figure 6: Velocity Magnitude Contour in 2D View of the (a) Model 1 ($\beta = 15^\circ$), (b) Model 2 ($\beta = 30^\circ$) and (c) Model 3 ($\beta = 60^\circ$)

B Pressure Results

Figure 7 illustrates the relationship of pressure (pressure loss) with different angles of stenosed bifurcated artery. The results show that pressure was distributed on the wall of the artery and varies along the distance from inlet to the outlet region. The value of pressure is indicated by the bar color on the right of the each model in Figure 7. An important observation is that the lowest pressure value was found at the throat of the stenoses compared to other regions. The pressure started with a high pressure at the inlet region of the artery and rapidly dropped at the upstream of the stenosis till the throat is reached. This happened due to flow acceleration (velocity increases); however, after it passed through this location, pressure was forced to be recovered due to flow deceleration. Then, pressure immediately rose as it passed through the downstream of stenosed portion. Still, pressure was not achieved as the initial value was as before, having a low value, as it reached the outlet of the artery due to the assumption of pressure point constraint in the boundary condition. Besides, the increasing angle of stenosed bifurcated artery will result in an increased pressure in the mother artery. The results of a 15-degree angle effect in Figure 7 (a) shows the lowest pressure compared to others. In addition, a slight increase of 30 degrees of angle effect increased the pressure results in Figure 7 (b). Figure 7 (c) further supports that the increase in the number of angle at 60 degrees shows the severe increase of pressure level. Figure 7 (a) (b) and (c) further explain that different angles of stenosed bifurcated artery affect pressure magnitude. As the severity of the angle of degree increases, pressure increases and might cause changes in blood flow pressure in human artery.

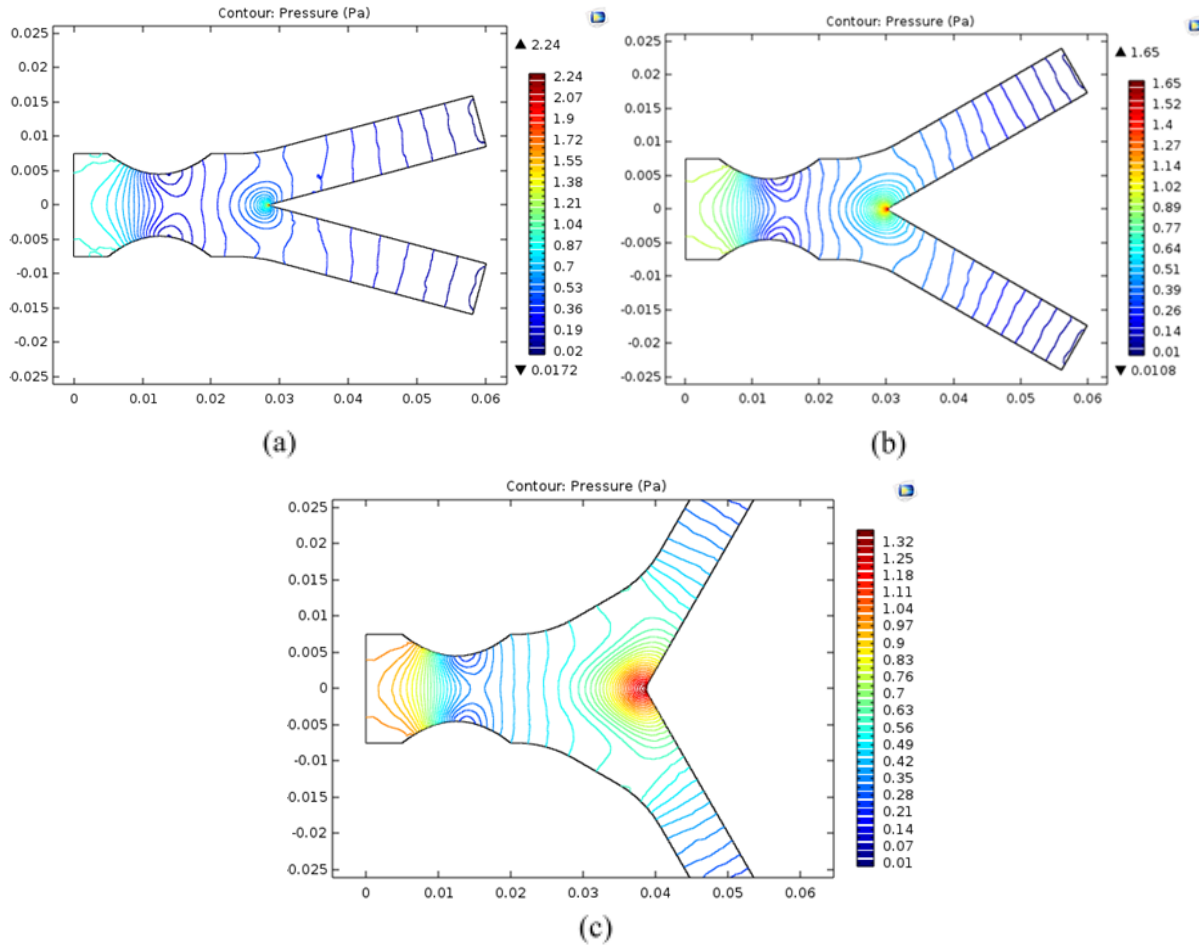


Figure 7: Pressure Results of the (a) Model 1 ($\beta = 15^\circ$); (b) Model 2 ($\beta = 30^\circ$); and (c) Model 3 ($\beta = 60^\circ$)

C Streamlines pattern for different severity of stenosis.

The influence of different bifurcation angles on the flow recirculation zones are illustrated in Figures 8-10 for severity $\beta = 15^\circ$, 30° , 60° , respectively. Overall, the recirculation zone appears at the offset of the stenosis for all models. Clearly, several flow lines were attracted towards the stenotic wall downstream with the formation of recirculation zones. As the reversed flow of the vortex reaches the edge of stenosis, it is unable to follow the curve of stenosis and to move away by changing its direction at the same time (refer to the big arrows pointing at specific areas (Figures 8-10)). As the bifurcation angle increases, the flow reversal and recirculation zones are formed and become severe, which might expose an individual to a worsening effect of cardiovascular disease.

Figure 8 further explains that the streamline pattern for geometry at $\beta = 15^\circ$ shows a noticeable recirculation zones in the downstream region of stenosis compared to Figure 9, where the streamline pattern for an angle of stenosed bifurcated artery at 30 degrees of angle is increasing. The higher value of the angle of stenosed bifurcated artery will influence the severity on the flow recirculation zones as illustrated in Figure 10. Here, the angle of $\beta = 60^\circ$ shows an abnormal behaviour of streamline flows. Despite that, the circulation shows severe increase at the upper half of the bifurcated artery. In conclusion, increasing the angles of stenosed bifurcated artery will increase the flow of streamlines that lead to the increase of blood flow circulation. Hence, the severity of stenosis discovered can

enhance vortex formation and may lead to serious complications on flow characteristics and may also trigger plaque rupture into small particles, which then travel downstream to the smaller vessels. Here, the small vessels could be blocked totally, Stroud et al. [17] and Riahi et al. [18]. This is the reason an individual may suffer from stroke, heart attacks, and peripheral vascular disease, Huh [1].

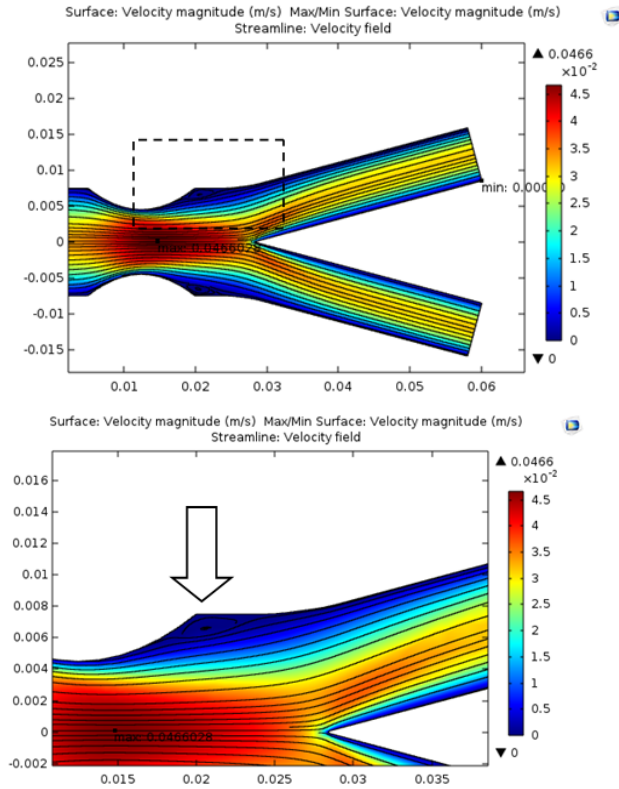
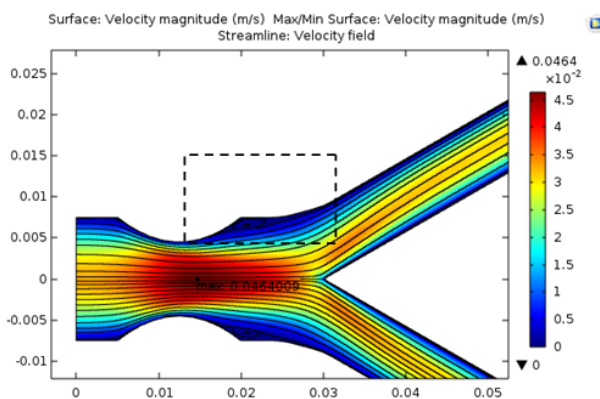
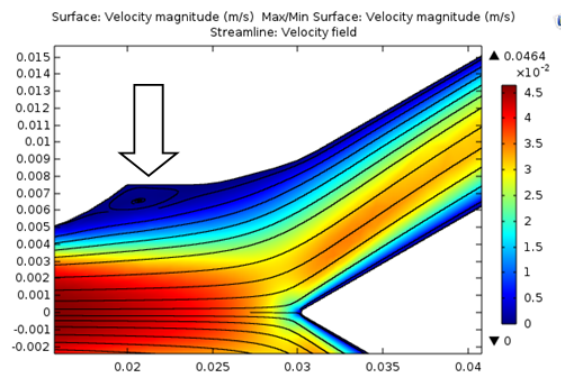
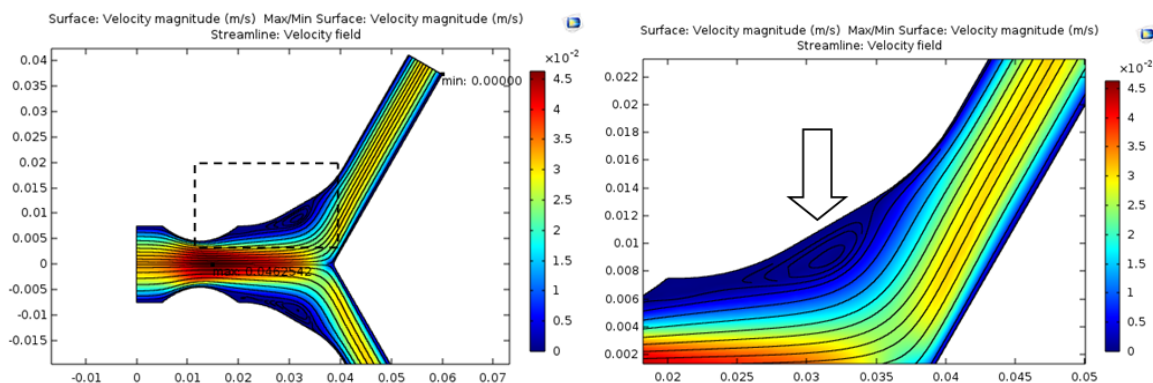


Figure 8: Streamline Patterns of Model 1 ($\beta = 15^0$)



Figure 9: Streamline patterns of model 2 ($\beta = 30^\circ$)Figure 10: Streamline patterns of model 1 ($\beta = 60^\circ$)

6 Conclusion

A mathematical model of a steady, laminar, incompressible, and generalized power law blood rheology in a stenotic bifurcated artery has been developed where the shape of the stenosis is considered mild. Results are generated using COMSOL Multiphysics 5.2 which shows that different angles of stenosed bifurcated artery produce different blood flow problems. The analysis was carried out to investigate the effects caused by the angles of stenosed bifurcated artery which resulted in the severity of velocity magnitude. As the severity of the angle of degree increases, pressure increases and might cause changes in the blood flow pressure in human artery. Increasing the angles of stenosed bifurcated artery increases flow of streamlines that lead to the increase in blood flow circulation and the condition of stenosed bifurcated artery. The salient observations of the present study found the increasing angles of stenosed bifurcated artery show an abnormal flow behavior and circulation was formed severed at the upper half of the bifurcated artery. As the reversed flow of the vortex reaches the edge of stenosis, it is unable to follow the curve of stenosis and to move away by changing its direction at the same time. The establishment of this study may provide better understanding in the behaviour of blood flow and this can be used for validation purposes against future experimental and numerical results.

Acknowledgements

The authors would like to acknowledge the Ministry of Higher Education and Research Management Centre, Universiti Teknologi Malaysia for the financial support. The authors are also grateful for the

support and hospitality of the Sydney Mathematical Research Institute (SMRI) and Griffith University. This work was supported by the Ministry of Higher Education [R.J130000.7854.5F255 (FRGS Grant)] and Research Management Centre, Universiti Teknologi Malaysia (UTM) [Q.J130000.2554.21H48 (UTMFR Grant)].

References

- [1] H. K. Huh, H. Ha and S. J. Lee, Effect of non-Newtonian viscosity on the fluid-dynamic characteristics in stenotic vessels, *Experiments in Fluids*, vol. 56, no. 8, pp. 1-12, 2015.
- [2] N. M. Zain and Z. Ismail, Modelling of Newtonian blood flow through a bifurcated artery with the presence of an overlapping stenosis, *Malaysian Journal of Fundamental and Applied Sciences*, vol. 13, no. 2017, pp. 304–309, 2017.
- [3] A. Zaman, N. Ali, M. Sajid, T. Hayat, Effects of unsteadiness and non-Newtonian Rheology on blood flow through a tapered time-variant stenotic artery. *AIP Advances*. vol 5, no. 3, pp. 0371291- 03712913, 2015.
- [4] L. Genuardi, Y. S. Chatzizisis, C. Chiastra, G. Sgueglia, H. Samady, G. S., Kassab,... and F. Burzotta, Local fluid dynamics in patients with bifurcated coronary lesions undergoing percutaneous coronary interventions, *Cardiology Journal*, 2020.
- [5] D. N. Ku, 'Blood flow in arteries', *Annual Review of Fluid Mechanics*, vol. 29, no. 1, 1974.
- [6] M.G. Rabby, S.P. Shupti and M.M Molla, Pulsatile Non-Newtonian Laminar Blood Flows through Arterial Double Stenoses. *Journal of Fluids*, vol. 2014, no. 757902, pp. 1-13, 2019.
- [7] B. M. Johnston, P. R. Johnston, S. Corney and D. Kilpatrick, Non-Newtonian blood flow in human right coronary arteries: steady state simulations, *Journal of Biomechanics*, vol. 37 no. 5, pp. 709-720, 2004.
- [8] Sarifuddin, S. Chakravarty, & P. K. Mandal,, Effect of asymmetry and roughness of stenosis on non-Newtonian flow past an arterial segment, *International Journal of Computational Methods*, vol. 6, no. 03, pp. 361-388, 2009.
- [9] S. V. H. N. K. Kumari, M. V. Murthy, M. C. K. Reddy and Y. V. K. R. Kumar, Peristaltic pumping of a magnetohydrodynamic Casson fluid in an inclined channel, *Adv. Appl. Sci. Res*, vol. 2, no. 2, pp. 428-436, 2011.
- [10] D. Biswas and M. Paul, Study of blood flow inside an inclined non-uniform stenosed artery, *International Journal of Mathematical Archive*, vol. 4, no. 5, pp. 33-42, 2013.
- [11] S. R. Verma and A. Srivastava, Effect of magnetic field on steady blood flow through an inclined circular tube, *International Journal of Engineering Research and Applications*, vol. 3, no. 4, pp. 428-432, 2013.

- [12] D. Biswas and M. Paul, Suspension model for blood flow through a tapering catheterized inclined artery with asymmetric stenosis, *Applications & Applied Mathematics*, vol .10, no.1, 2015.
- [13] M. S. A. Jamali and Z. Ismail, Generalized power law model of blood flow in a stenosed bifurcated artery, *Annals of Mathematical Modeling*, vol. 1, no. 2, pp. 35-46, 2019.
- [14] S. Chakravarty and P. K. Mandal, An analysis of pulsatile flow in a model aortic bifurcation, *International Journal of Engineering Science*, vol. 35, no. 4, pp. 409-422, 1997.
- [15] L. Zain and Z. Ismail, Modelling of Newtonian blood flow through a bifurcated artery with the presence of an overlapping stenosis, *Malaysian Journal of Fundamental and Applied Sciences Special Issue on Some Advances in Industrial and Applied Mathematics* pp. 304-309, 2017.
- [16] D. Srinivasacharya and G. M. Rao, Modeling of blood flow through a bifurcated artery using nanofluid, *BioNanoScience*, vol. 7, no. 3, pp. 464-474, 2017.
- [17] J. S. Stroud, S. A. Berger and D. Saloner, Numerical analysis of flow through a severely stenotic carotid artery bifurcation, *J. Biomech. Eng.*, vol. 124, no. 1, pp. 9-20, 2002.
- [18] D. N. Riahi, R. Roy and S. Cavazos X, On arterial blood flow in the presence of an overlapping stenosis, *Mathematical and Computer Modelling*, Vol. 54, no. 11-12, pp. 2999-3006, 2011.